

## 1. Introduction

This summer, my work focused on building and testing a panoramic vision system using a conical mirror, based on our lab's SKOOTR platform. Since SKOOTR can move in any direction at any time, it needs a vision system that can also "see" in all directions for tasks like line patrol or obstacle detection, without having to physically rotate the camera or adding multiple redundant cameras.

To address this, I experimented with a catadioptric setup using a 3D-printed conical mirror polished with chrome powder and a single Logitech C920 Webcam. My work had four main parts: (1) Previous Work, where I reviewed papers on omnidirectional vision and unwarping strategies, (2) Theory, where I derived formulas tailored to ground-looking geometry, (3) Hardware, where I designed, printed, and tested different cone mirror prototypes, and (4) Software, where I built unwarping functions in OpenCV and calibrated the outputs.

In this summary, I will present all the work I carried out over the summer, along with the results, challenges I encountered and suggestions for future improvements.

## 2. Previous Work

To guide my work, I reviewed several papers on catadioptric imaging and conical mirrors.

### ***Baker & Nayar (1999) A Theory of Single-Viewpoint Catadioptric Image Formation***

- SVP is the requirement for catadioptric sensors; this paper describes all of the solutions(rotated conic sections).
- Derived fixed SVP constraint equation, solutions are planar, conical, spherical, ellipsoidal, and hyperboloidal.
- For conical mirrors, the pinhole of the camera must be at the apex of the cone, which is thus a degenerate solution.
- The circular locus lies on the cone only if the cone tip angle is 60 degrees.
- Derived the resolution mapping equation for hyperboloidal and ellipsoidal mirrors, should apply to conical mirrors but might not be very robust (worth giving it a try).
- Blurring analysis for hyperboloidal and ellipsoidal mirrors.

### ***Yagi et al. (1994) Real-time omnidirectional image sensor (COPIS) for vision-guided navigation***

- Conical mirror + TV camera aligned with the cone's axis.
- Small aperture and short focal length lens.
- Installed on the robot for collision detection.
- Use trajectories of vertical edges over time as well as the azimuth direction(the angle of the robot towards the object), to compute the direction of relative motion.
- All computations in polar coordinates, no unwarping.

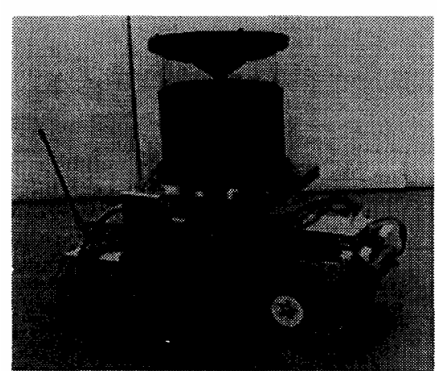
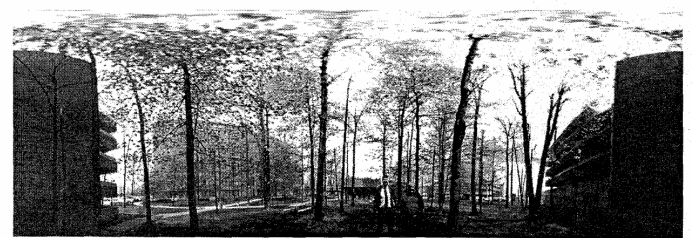


Fig. 12. A prototype of the conic projection image sensor (COPIS).

**Bogner (1995) An Introduction to Panospheric Imaging**

- They aim to capture a spherical field of view (360° horizontal + ≥ 180° vertical).
- Fisheye lenses + spherical/conical mirrors.
- Image Transformation Engine: LUT for pixel address imaging.



**Lin & Bajcsy (2006) Single-viewpoint, catadioptric cone mirror omnidirectional imaging theory and analysis**

- They proved that a conical mirror can still create SVP, which contradicts Baker & Nayar (1999).
- They provided the experiment setup in Lin & Bajcsy (2001).
- Conical mirror
  - a. Top angle approx. 90-110
- Camera
  - a. Fixed aperture for Logi C920
  - b. Need to disable auto focus with Logitech capture
- Position
  - a. Need pixel focal length, already retrieved with calibrateCamera() from opencv
  - b. Might not get the datasheet for CMOS
- Calculations
  - a. Vertical FOV of the camera
  - b. Horizontal FOV of the camera
- Minimizing Aberration Effects
  - a. Change F/Number: Best at F/16 (at diffraction limit)
  - b. Move the aperture: The farther away from the lens, the better. Restricted by vignetting.
  - c. Best at F/16 with 4.865 backwards.
  - d. Change mirror shapes: The smaller the tip angle, the better. Needs to consider FOV.
  - e. Change focal length: The shorter the f, the better.
  - f. Change mirror size: Doesn't matter. Just make sure sufficient FOV.
- Experiments
  - a. SVP conditions are much more robust to longitudinal errors than lateral errors.
  - b. It can move up and down on the optical axis direction, but must be aligned with the tip.
  - c. F/2 works badly, F/10 works great.

- d. A standard digital camera works well at 1/30s exposure.

***Swaninathan et al. (2003) A perspective on distortions***

- SVP (and approximate) can be undistorted perfectly, including a conical mirror.
- In terms of undistortion algorithms, they only derived ones for MVI (Multi-Viewpoint Image).
- Undistorting MVI requires a simple geometry primitive, with a basic uncertainty model for parameters.
- Proposed a metric to quantify distortions relative to a true perspective view.

***Ward (1965) Optical Properties and Uses of the Conical Mirror***

- Concave conical mirror.
- Analysis suggests not strictly SVP, but can approximate it in certain configurations.
- Derived relation between cone angle and magnification, focused on the geometric reference at the design level.

***Lin & Bajcsy (2001) True single view point cone mirror omni-directional catadioptric system***

- Provided the experiment setup in Fig. 8, with a m12 s-mount lens.
- Provided a detailed unwarping algorithm in Section 4.
- Removing a small amount from the tip does not affect the geometry, but only slightly affects the brightness.

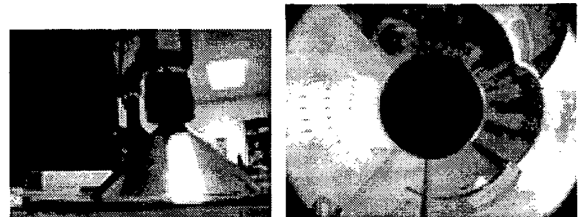


**Figure 8** The tip of the cone actually coincides with the effective pinhole. Right: cone omni-view seen by the camera. The left side is a test pattern with dots 4" apart.

### 3. Background & Theoretical Formulation

#### a. Single Viewpoint Property (SVP)

For catadioptric imaging, SVP means all reflected rays pass through a single effective viewpoint, in our case, the cone tip, making it possible to map images back to perspective without distortion. Conical mirrors are theoretically a degenerate SVP case (Baker & Nayar, 1999), but later works (Lin & Bajcsy, 2006) still showed that approximate SVP should still work in practical use. In our setup, approximate SVP can be achieved by aligning the cone and camera using the entrance pupil, which we determine with the parallax method (described in the Hardware Setup section).

#### b. Unwarping Algorithm

Standard omnidirectional vision systems typically transform cone or spherical mirror images into panoramas by converting from image coordinates  $(r, \theta)$  in

polar space to planar coordinates (X, Y). Formulas are given in Lin & Bajcsy (2006).

c. Our Unwarping Algorithm

Most previous work on catadioptric vision with conical mirrors has focused on capturing the surroundings of a robot. In contrast, our design is designed for SKOOTR, where the camera looks upward into a cone mirror that reflects the ground plane. This different geometric reasoning requires new formulas to map the mirror image back to real-world coordinates. The new formulas will be presented in *Appendix III*.

#### 4. Hardware Setup

The hardware setup, as shown in the figures below, consists of an upward-facing camera and a downward-pointing conical mirror mounted along a common optical axis. This arrangement enables the camera to capture a complete panoramic view of the ground through the mirror's reflective surface.



Figure 1: Side view of the setup



Figure 2: Top view of the hardware setup over the floor

We designed and fabricated the cone mirror ourselves, as commercial conical mirrors are costly (~ \$600 each). The mirror was 3D-printed with resin material (to ensure smoothness) and then polished with chrome powder to create a reflective surface. I experimented with multiple prototypes that varied in height, radius, and tip angle, ultimately using a 126.8° tip angle. This geometry provided a wide field of view while maintaining acceptable reflection quality for ground-looking imaging.

A Logitech C920 webcam is mounted beneath the mirror, facing upward. The camera's optical axis is aligned with the mirror's centerline, and its position is adjusted such that the entrance pupil lies approximately on the cone's axis. The entrance pupil location was determined experimentally using the parallax (two-pen) method, which minimizes relative motion between near and far reference objects during camera rotation. To measure the position of the entrance pupil:

1. Mount the camera on a rotation stage aligned with its optical axis.
2. Place one reference pen close to the camera and another several meters away.
3. Rotate the camera slightly about the pivot axis.
4. Adjust the camera's position along the rail until the near and far pens remain aligned during rotation.
5. Record this position as the entrance pupil for the current lens configuration.

To evaluate the unwarping accuracy, a sheet of paper with grids was placed flat on the floor. Images of this pattern were captured using the cone-mirror setup. The resulting image was then processed with the unwarping algorithm to verify geometric correctness. A sample raw image and its corresponding unwarped result are presented in the results section for comparison.

## 5. Software & Image Processing

As noted in Section 2 and based on the approach described by Lin and Bajcsy (2006), it is essential that the center of the captured image aligns precisely with the cone tip. To achieve this, an initial calibration process was implemented using a Python script that overlays a red dot at the center of the live video stream. This visual guide assists in adjusting both the camera position and mirror alignment to ensure that the cone's apex corresponds to the exact center of the image.

After centering, the orientation of the mirror is verified. The visible rim of the cone is detected using OpenCV's Hough Circle Transform (`cv2.HoughCircles()`), and a circle is drawn with `cv2.circle()` to visualize the boundary. The boundary identification is illustrated in Figure 3 below. The geometric center of this detected circle is then compared to the red reference point in the video stream. Adjustments are made until the two points coincide, ensuring that the mirror is level and its axis coincides with the camera's optical axis.



Figure 3: Calibration view showing the detected mirror boundary (green circle) and the red reference point at the center

Once the calibration was completed, the unwarping process was applied. Using the derived geometric relationships and transformation equations (presented in Appendix III), the raw circular mirror image was converted into a flat panoramic projection. This transformation enables the system to accurately represent the ground plane for navigation and analysis tasks.

## 6. Results

The results of the unwarping process are illustrated below. Figure 4 shows the original mirrored image captured from the upward-facing camera, displaying the ground reflection in its raw circular form. Figure 5 demonstrates the output from our custom unwarping algorithm, which produces a more geometrically accurate representation of the ground plane with significantly reduced distortion and improved scale uniformity across the panorama.

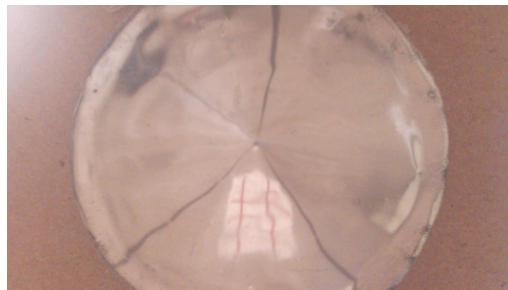


Figure 4: Raw circular mirrored image from the upward-facing camera



Figure 5: Unwarped panoramic view of the ground produced by the algorithm

## 7. Challenges, Lessons, and Future Suggestions

One of the main challenges encountered during this project was the mechanical alignment between the camera and the cone mirror. Since the support structure was improvised using simple materials such as chopsticks rather than a 3D-printed or machined mount, maintaining precise coaxial alignment proved difficult. Even small angular deviations between the camera's optical axis and the cone's axis caused noticeable asymmetry in the captured image, making calibration and unwarping less reliable.

Another difficulty was achieving a stable and repeatable mounting configuration. The lightweight materials tended to shift slightly during adjustment, which affected the mirror's height and orientation. As a result, each calibration required fine manual readjustment, especially when

ensuring that the cone's tip aligned exactly with the image center and that the rim formed a perfect circle.

Additionally, surface quality and lighting posed challenges. The polished PLA mirror surface, while reflective, was not perfectly smooth, introducing scattering and uneven brightness across the image. Ambient light variations and reflections from surrounding objects also interfered with accurate edge and circle detection during software calibration.

Lastly, the unwarping process was sensitive to small measurement errors in the cone angle and the camera–cone distance ( $h$ ). Inaccurate physical measurements or lens refocusing would alter the geometry slightly, requiring recalibration before reliable panoramic reconstruction could be achieved.

## 8. Conclusion

In this project, I designed, built, and tested a conical-mirror catadioptric vision system for SKOOTR that can capture and unwarped a full panoramic view of the ground using a single upward-facing camera. Through reviewing prior work, deriving ground-looking unwarping formulas, fabricating and aligning a custom cone mirror, and implementing a calibration and unwarping pipeline in OpenCV, I demonstrated that this approach can produce usable, approximately geometrically correct panoramas from low-cost hardware. While mechanical alignment, mirror quality, and sensitivity to geometric parameters still limit accuracy and repeatability, these issues can be addressed with a rigid 3D-printed mount, higher-quality optics, and more automation in calibration. Overall, the system provides a promising starting point for future work on real-time ground-plane perception and navigation on the SKOOTR platform.

## 9. Appendix

### Appendix I: All Python codes

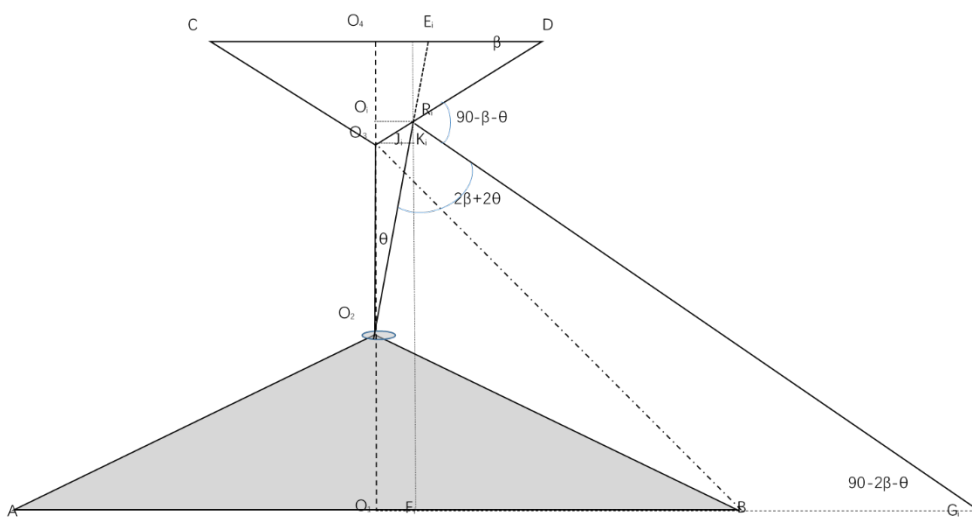
Python codes implementing the unwarping algorithms and the boundary detections can be found in this Google Drive folder: [Cone mirror codes](#)

### Appendix II: SKOOT's URDF & simulation files

URDF and simulation files can be found in this GitHub repository: [Github](#)

All other files can be found in this Dropbox folder: [Dropbox](#)

### Appendix III: Formulae for Ground Plane Unwarping Algorithms



Any incident ray  $O_2R_i$ , striking the cone surface  $O_3D$  at point  $R_i$ , is reflected as  $RG_i$ , reaching the ground at point  $G_i$ ; Needs to calculate the length of  $O_1G_i$ :

$$O_1G_i = \mathbf{O}_1\mathbf{F}_i + \mathbf{F}_i\mathbf{G}_i \quad (1)$$

$$O_1F_i = O_iR_i = O_3J_i + J_iK_i = O_2O_3 \tan \theta + J_iK_i = \mathbf{O}_2\mathbf{O}_3 \tan \theta + \mathbf{R}_i\mathbf{K}_i \tan \theta \quad (2)$$

$$R_iK_i = O_iO_3 = \mathbf{O}_i\mathbf{R}_i \tan \beta \quad (3)$$

$$(3) \text{ substituting into (2) gives: } O_iR_i = O_2O_3 \tan \theta + R_iK_i \tan \theta = \mathbf{O}_2\mathbf{O}_3 \tan \theta + \mathbf{O}_i\mathbf{R}_i \tan \beta \tan \theta \quad (4)$$

$$O_2O_3 \text{ is known, } O_iR_i \text{ can be determined from equation (4): } O_iR_i = \frac{\mathbf{O}_2\mathbf{O}_3 \tan \theta}{1 - \tan \beta \tan \theta} \quad (5)$$

$$\text{From (3) and (5), } R_iK_i = O_iR_i \tan \beta = \left( \frac{\mathbf{O}_2\mathbf{O}_3 \tan \theta}{1 - \tan \beta \tan \theta} \right) \tan \beta = \frac{\mathbf{O}_2\mathbf{O}_3 \tan \theta \tan \beta}{1 - \tan \beta \tan \theta} \quad (6)$$

$$\text{From } \Delta R_iF_iG_i \text{ we have } F_iG_i = R_iF_i \tan(90 - 2\beta - \theta) = (R_iK_i + K_iF_i) \tan(90 - 2\beta - \theta) = \left( \frac{\mathbf{O}_2\mathbf{O}_3 \tan \theta \tan \beta}{1 - \tan \beta \tan \theta} + \mathbf{O}_2\mathbf{O}_3 + \mathbf{O}_2\mathbf{O}_1 \right) \cot(2\beta + \theta) \quad (7)$$

$$\mathbf{O}_1\mathbf{G}_i = O_1F_i + F_iG_i = O_iR_i + F_iG_i = \left( \frac{\mathbf{O}_2\mathbf{O}_3 \tan \theta}{1 - \tan \beta \tan \theta} \right) + \left( \frac{\mathbf{O}_2\mathbf{O}_3 \tan \theta \tan \beta}{1 - \tan \beta \tan \theta} + \mathbf{O}_2\mathbf{O}_3 + \mathbf{O}_2\mathbf{O}_1 \right) \cot(2\beta + \theta) =$$

$$\mathbf{O}_2\mathbf{O}_3 \frac{\tan \theta(1 + \tan \beta \cot(2\beta + \theta))}{1 - \tan \beta \tan \theta} + (\mathbf{O}_2\mathbf{O}_3 + \mathbf{O}_2\mathbf{O}_1) \cot(2\beta + \theta) = \mathbf{O}_2\mathbf{O}_3 \frac{\tan \theta(1 + \tan \beta \cot(2\beta + \theta))}{1 - \tan \beta \tan \theta} + (\mathbf{O}_3\mathbf{O}_1) \cot(2\beta + \theta) \quad (8)$$

From equation (8), it can be seen that  $O_1O_2$  represents the height of the robot,  $O_2O_3$  represents the height of the vertex of the panoramic conical mirror relative to the installation point,  $O_1O_3$  represents the height of the vertex of the conical mirror, and  $\beta$  is the complementary angle of the cone angle of the conical mirror, all of which are known quantities.  $\theta$  is the variable.



Along the horizontal y-direction (perpendicular to the optical axis), an obstacle located at  $G_i$  with the width  $G_iG_i'$  forms a circular image; the circle size corresponds to the radius  $O_iR_i$  associated with the incident angle  $\theta$  in the previous figure. The image of the obstacle of width  $G_iG_i'$  is  $O_iO'_i$ , whose magnitude is computed as follows:

The radial incident angle for the obstacle of width  $G_iG_i'$  is  $\phi_i$ , which is computed as follows:

$$\varphi_i = \sin^{-1} \left( \frac{G_i G'_i}{O_i R_i} \right) = \sin^{-1} \left( \frac{G_i G'_i}{(O_2 O_3 \tan \theta / 1 - \tan \beta \tan \theta)} \right) \quad (9)$$

$$O_i O'_i = O_i M'_i \tan \Delta O_i M'_i O'_i = O_i M'_i \tan 2\varphi_i = \left( \frac{\frac{O_i R_i}{2}}{\cos \varphi_i} \right) \tan 2\varphi_i = \left( \left( \frac{O_2 O_3 \tan \theta}{1 - \tan \beta \tan \theta} \right) / 2 \cos \varphi_i \right) \tan 2\varphi_i = \frac{\left( \frac{O_2 O_3 \tan \theta}{1 - \tan \beta \tan \theta} \right) \tan 2\varphi_i}{2 \cos \varphi_i} \quad (10)$$

$$O_i O'_i = \frac{\left( \frac{O_2 O_3 \tan \theta}{1 - \tan \beta \tan \theta} \right) \tan 2\varphi_i}{2 \cos \varphi_i} = \frac{\left( \frac{O_2 O_3 \tan \theta}{1 - \tan \beta \tan \theta} \right) \sin 2\varphi_i}{2 \cos \varphi_i \cos 2\varphi_i} = \frac{\left( \frac{O_2 O_3 \tan \theta}{1 - \tan \beta \tan \theta} \right) 2 \sin \varphi_i \cos \varphi_i}{2 \cos \varphi_i (1 - 2(\sin \varphi_i)^2)} = \frac{\left( \frac{O_2 O_3 \tan \theta}{1 - \tan \beta \tan \theta} \right) \sin \varphi_i}{(1 - 2(\sin \varphi_i)^2)} \quad (11)$$

Substitute (9) into (11) gives

$$O_i O'_i = \frac{\left( \frac{O_2 O_3 \tan \theta}{1 - \tan \beta \tan \theta} \right) \sin \varphi_i}{(1 - 2(\sin \varphi_i)^2)} = \frac{\left( \frac{O_2 O_3 \tan \theta}{1 - \tan \beta \tan \theta} \right) \left[ \frac{G_i G'_i}{\left( \frac{O_2 O_3 \tan \theta}{1 - \tan \beta \tan \theta} \right)} \right]}{\left( 1 - 2 \left( \frac{G_i G'_i}{\left( \frac{O_2 O_3 \tan \theta}{1 - \tan \beta \tan \theta} \right)} \right)^2 \right)} = \frac{G_i G'_i}{1 - 2 \left( \frac{G_i G'_i}{O_2 O_3} \right) \left( \frac{1 - \tan \beta \tan \theta}{\tan \theta} \right)^2} \quad (12)$$

From equation (12),  $O_2 O_3$  represents the height of the vertex of the panoramic conical mirror relative to its installation point,  $G_iG_i'$  represents the horizontal width of the obstacle,  $\beta$  is the complementary angle of the cone angle of the conical mirror; all of these are known quantities.  $\theta$  is the variable. Thus for any direction  $\theta$ , the conical image width of the obstacle with horizontal width  $G_iG_i'$  is  $O_iO'_i$ .

